Cerebral Cortex June 2006;16:811-818
doi:10.1093/cercor/bhj024
Advance Access publication August 24, 2005

The Evolution of Prefrontal Inputs to the Cortico-pontine System: Diffusion Imaging Evidence from Macaque Monkeys and Humans

Narender Ramnani[1,2], Timothy E.J. Behrens[2], Heidi Johansen-Berg[2], Marlene C. Richter[3,4], Mark A. Pinsk[3,4], Jesper L.R. Andersson[5], Peter Rudebeck[1], Olga Ciccarelli[6], Wolfgang Richter[3,7], Alan J. Thompson[6], Charles G. Gross[4], Matthew D. Robson[8], Sabine Kastner[3,4] and Paul M. Matthews[2]

[1]Cognitive Neuroscience Laboratory, Department of Psychology, Royal Holloway University of London, UK, [2]Centre for Functional Magnetic Resonance Imaging of the Brain (FMRIB), University of Oxford, Oxford, UK, [3]Centre for the Study of Mind, Brain and Behavior, Princeton University, Princeton, NJ, USA, [4]Department of Psychology, Princeton University, Princeton, NJ, USA, [5]Karolinska MR Research Centre, Karolinska Institute, Stockholm, Sweden, [6]Department of Headache, Brain Injury and Neurorehabilitation, Institute of Neurology, University College London, London, UK, [7]Department of Chemistry, Princeton University, Princeton, NJ, USA and [8]Centre for Clinical Magnetic Resonance Imaging (OCMR), University of Oxford, Oxford, UK

The cortico-ponto-cerebellar system is one of the largest projection systems in the primate brain, but in the human brain the nature of the information processing in this system remains elusive. Determining the areas of the cerebral cortex which contribute projections to this system will allow us to better understand information processing within it. Information from the cerebral cortex is conveyed to the cerebellum by topographically arranged fibres in the cerebral peduncle — an important fibre system in which all cortical outputs spatially converge on their way to the cerebellum via the pontine nuclei. Little is known of their anatomical organization in the human brain. New *in vivo* diffusion imaging and probabilistic tractography methods now offer a way in which input tracts in the cerebral peduncle can be characterized in detail. Here we use these methods to contrast their organization in humans and macaque monkeys. We confirm the dominant contribution of the cortical motor areas to the macaque monkey cerebral peduncle. However, we also present novel anatomical evidence for a relatively large prefrontal contribution to the human cortico-ponto-cerebellar system in the cerebral peduncle. These findings suggest the selective evolution of prefrontal inputs to the human cortico-ponto-cerebellar system.

Keywords: cerebellum, diffusion imaging, macaque, pontine nuclei, prefrontal cortex

Introduction

It has been suggested that the cortico-ponto-cerebellar system is comprised of a set of parallel, closed-loop pathways in which the cerebral cortex projects to the cerebellum via the cerebral peduncle and the pontine nuclei, and in which the cerebellum returns projections to the cortex via the thalamus (Middleton and Strick, 2000). Two such loops have been particularly well characterized in the macaque monkey. In the 'motor loop', the primary motor cortex (BA4) and premotor cortex (BA6) project to the dorsal part of the dentate nucleus (the largest of the cerebellar nuclei) (Glickstein *et al.*, 1985; Orioli and Strick, 1989). In non-human primates, motor areas of the cerebral cortex form the principal cortical inputs to the ponto-cerebellar system (Glickstein *et al.*, 1985) and this system plays an important for the control of movement in humans and non-human primates (Glickstein, 1993; Brodal and Bjaalie, 1997).

In the less prominent 'prefrontal loop', prefrontal projections to the macaque monkey cerebellum arise mainly from area 9/46 in tissue dorsal to the upper bank of *sulcus principalis* (Glickstein *et al.*, 1985; Schmahmann and Pandya, 1995; Kelly and Strick, 2003) and project to ventral parts of the dentate nucleus (Middleton and Strick, 1994, 1997, 2001). Indirect evidence suggests that this specific pathway is much larger in the human brain. First, the cerebellum and the prefrontal cortex both have evolved rapidly relative to other brain structures (Zilles *et al.*, 1988, 1989; Finlay and Darlington, 1995; Rilling and Insel, 1998). Second, the ventral dentate (recipient of prefrontal inputs) has expanded much more than the dorsal dentate (recipient of cortical motor inputs) (Dow, 1942; Matano, 2001; Kelly and Strick, 2003). The 'Mosaic' hypothesis of brain evolution (Barton and Harvey, 2000) suggests that selectional pressures act on interconnected brain systems as a whole. Thus, there should also have been a parallel expansion of the pathways linking the cerebellum and the prefrontal cortex.

A direct test of this hypothesis can come from evaluating the relative contributions of prefrontal and motor loops to cortico-pontine fibres in the cerebral peduncle in both humans and non-human primates. Diffusion tensor magnetic resonance imaging (DT-MRI) has made it possible to conduct *in vivo* investigations of white matter projections in the brain. Fibre trajectories have been defined from origin to termination (Behrens *et al.*, 2003a,b) that agree well with conventional anatomical methods (Johansen-Berg *et al.*, 2004, 2005).

We used DT-MRI tractography to assess the relative contributions of seven cerebral cortical areas to fibres in the cerebral peduncle in nine humans and two macaque monkeys, and compared the relative contribution of prefrontal and motor projections in the cortico-pontine system in the same brains in both species using the same methods.

Degeneration studies suggest a well-organized topography of fibres in the cerebral peduncle (Beck, 1950; Marin *et al.*, 1962; Schultz *et al.*, 1976). We therefore predicted that our tractographic methods would segment the cerebral peduncle into topographically arranged fibre groups on the basis of their

origins in the cerebral cortex. Also, hypothesizing that selectional pressures act on systems as a whole, we predicted that the proportion of fibres originating from the prefrontal cortex would be substantially larger in humans than in macaque monkeys.

Materials and Methods

Image Acquisition

Human Cases

Diffusion-weighted data were acquired from nine healthy subjects (six male, ages 26–33 years) using echo planar imaging [60 2.3 mm thick slices, field of view (FOV) = 220 × 220 mm^2, matrix = 96 × 96; images were reconstructed on a 128 × 128 matrix giving a final resolution of 1.7 × 1.7 × 2.3 mm^3] implemented on a General Electric 1.5 T Signa Horizon scanner with a standard quadrature head-coil and maximum gradient strength of 22 mT/m. Informed written consent was obtained from all subjects in accordance with ethical approval from the National Hospital for Neurology and Neurosurgery and Institute of Neurology joint research ethics committee. The diffusion weighting was isotropically distributed (Jones *et al*., 1999) along 54 directions (δ = 34 ms, Δ = 40 ms, *b*-value = 1,150 s/mm). Six additional diffusion-weighted volumes (*b*-value = 300 s/mm) and six volumes with no diffusion weighting were acquired. Cardiac gating (Wheeler-Kingshott, 2002) was used to minimize artefacts from pulsatile flow of the cerebrospinal fluid. The total scan time for the diffusion-weighted imaging (DWI) protocol was ~20 min (depending on heart rate).

High-resolution T1-weighted scans were obtained with a three-dimensional inversion recovery prepared spoiled gradient echo (IR-SPGR) (FOV = 310 × 155; matrix = 256 × 128; in-plane resolution = 1.2 × 1.2 mm^2; 156 × 1.2 mm thick slices; T_I = 450 ms; T_R = 2 s; T_E = 53 ms).

Macaque Monkey Cases

MR images were acquired from two adult male macaque monkeys (*Macaca fascicularis*). All procedures were approved by the Princeton University Animal Care and Use Committee and conformed to NIH guidelines for the humane care and use of laboratory animals. Surgical procedures for the monkeys were performed under strictly aseptic conditions and under general anaesthesia with isoflurane (induction, 2–4%; maintenance, 0.5–2%) following preanaesthetic medication with atropine (0.08 mg/kg i.m.), ketamine (2–10 mg/kg i.m.) and acepromazine (1 mg/kg). In these animals, a plastic head bolt for restraining the head was implanted to extend vertically from the rostral cranium using ceramic screws (ZrO_2 + Y_2O_3) and dental acrylic (Pinsk *et al*., 2005). The animals were treated post-surgically with antibiotics (e.g. Baytril, 2.5 mg/kg i.m.) and analgesics (e.g. Buprenorphine, 0.01 mg/kg i.m.). Wound margins of skin surrounding the implant were cleaned regularly.

During the imaging sessions, monkeys were placed in the 'sphinx' position in an MR-compatible primate chair (Pinsk *et al*., 2005). A polyetherimide head post, attached to the implanted head bolt of each monkey, was secured to the primate chair to achieve rigid head fixation. The animals were anesthetized with Telazol (tiletamine/zolazepam, 10 mg/kg i.m.) during scanning.

Images were acquired with a 3 Tesla head-dedicated horizontal bore MR scanner (Magnetom Allegra; Siemens Medical, Erlangen, Germany). A 12 cm surface coil (Model NMSC-023; Nova Medical Inc., Wakefield, MA) was used for radio frequency transmission and reception. The coil was secured to the head restraint system of the MR-compatible primate chair with two plastic C-clamps above the animal's head.

For each animal, a high resolution (1.0 × 0.5 × 0.5 mm) 3D MPRAGE structural scan was acquired (FOV = 128 × 128 mm; 256 × 256 matrix; 1.0 mm slice thickness; T_R = 2500 ms; T_E = 4.4 ms; T_I = 1100 ms; flip angle = 8°; 130 Hz/pixel bandwidth). Diffusion-weighted images were collected using a double spin-echo EPI readout pulse sequence. Images with 1.0 × 1.0 × 1.0 mm resolution were collected using 60 different isotropic diffusion directions [45 slices without any gap; FOV = 128 × 96 mm; 128 × 96 matrix; 1.0 mm slice thickness; T_R = 10000 ms; T_E = 145 ms; 1 average; interleaved acquisition; two *b*-values of 0 and 1000 s/mm^2; 1056 Hz/pixel bandwidth; image acquisition time of 5′10″ for 29 directions and 5′30″ for 31 directions for full 60 direction set].

Image Preprocessing

Preprocessing Software

All image preprocessing was conducted using tools developed at the Centre for Functional Magnetic Resonance Imaging of the Brain (FMRIB Centre, University of Oxford). These are incorporated into the FMRIB Software Library (FSL; www.fmrib.ox.ac.uk/fsl). The preprocessing tools used included BET (Smith, 2002) used for automated scalp-editing of human brain images (macaque monkey images were edited manually), and FLIRT (Jenkinson *et al*., 2002) for image registration. Grey matter segmentation was conducted using FAST (Zhang *et al*., 2001).

Preprocessing Steps Common to Data from Human and Macaque Monkey Cases

Correction for eddy currents and motion: All diffusion- and non-diffusion-weighted images were registered to a non-diffusion-weighted reference image using affine (12 degrees of freedom) registration with a correlation ratio objective function.

Analysis was performed on diffusion-weighted images in their own native spatial frame of reference (DWI space). Thus, although masks of cortical areas of interest (see 'Preparation of anatomical masks' below) were constructed from T1-weighted images in which there was greater anatomical detail (T1-weighted anatomical frame of reference; T1 space), T1-weighted images were registered into DWI space using affine registration. The registration parameters were saved and later applied to register masks drawn in T1 space into DWI space.

Preprocessing Specific to Macaque Monkey Case

Images acquired from macaque monkey at 3 T field strength suffered more from susceptibility related distortions than images from human cases that were acquired at 1.5 T field strength. In order to correct for this difference, we submitted the macaque data to a previously described susceptibility distortion correction method (Andersson *et al*., 2004; Munger *et al*., 2000) which relies on the acquisition of two separate data sets with phase encode directions of opposite polarity. These suffer from distortions of the same magnitude but opposite directions. After correction for eddy currents and motion, we averaged all the diffusion-weighted volumes acquired with the same phase-encode polarity, thus obtaining one volume which was representative of the geometry as measured by each phase encode polarity. We used these two images to find the least squares estimate of the field, and then used this field to reconstruct undistorted versions of the original data.

Preparation Of Anatomical Mask Images

FSLView (FSL) and MRIcro (www.psychology.nottingham.ac.uk/staff/cr1/mricro.html) were used for image display and mask editing.

Segmentation of the Cerebral Peduncles

We manually created separate anatomical masks of the left and right cerebral peduncle in human cases, and in only the right cerebral peduncle in the macaque monkey cases (tractography was not conducted in the left hemispheres of the macaque monkeys because of artefacts caused by a post that was surgically affixed to the left half of the skull to facilitate scanning — see acquisition methods above). Masking is normally performed in the anatomical space defined by T1-wieghted anatomical images (T1 space) because of the high level of detail in these images. However, tractography analyses are conducted in the anatomical space defined by diffusion-weighted images (DWI space). Thus, prior to analysis anatomical masks defined in T1 space are registered into DWI space. While this procedure is reliable for most brain areas, others are sometimes prone to registration error. Inspection of the diffusion images revealed this to be negligible in the cerebral peduncles. Nevertheless, the structure of the cerebral peduncles was clearly visible in the diffusion images, and we therefore circumvented potential problems associated with registration between T1 and DWI space by defining masks of the cerebral peduncle in DWI space. Masking was conducted conservatively so as to avoid inclusion of adjacent

structures such as the optic nerve and temporal lobe (see Supplementary Material for criteria used).

Construction of Target Masks from Grey Matter Segmentation

Masks of the seven cortical areas of interest were constructed from grey matter identified in the T1 anatomical images. Grey matter was segmented from the brain by performing probabilistic tissue-type segmentation and partial volume estimation. Areas of cortex containing 35% or more grey matter were included in the grey matter mask. The grey matter areas were manually segmented into the seven cortical areas on the basis of sulcal and gyral landmarks (see Supplementary Material).

Diffusion Tractography

Tractography analysis was conducted using the FMRIB Diffusion Toolkit (FDT) (Behrens *et al.*, 2003b).

Probabilistic diffusion modelling and tractography were performed according to previously described methods (Behrens *et al.*, 2003a,b; Johansen-Berg *et al.*, 2004, 2005). Probability density functions (PDFs) were calculated by drawing 1000 samples from the projection distribution from the cerebral peduncle mask to each cortical mask, maintaining knowledge of location in structural and DWI spaces, and recording the proportion of these samples that passed into each of the cortical masks as the probability of projection to that zone. Prior pilot studies demonstrated that results ceased to differ from upwards of 750 samples. We therefore conservatively conducted analyses using 1000 samples.

This process established the probability of a projection between every voxel in the cerebral peduncle (source mask) and one of the seven target masks in the cerebral cortex. This information was used to express PDF information spatially where each voxel in the source mask was labelled with the probability of projection to the target mask. The process was repeated for each of the seven cortical target masks. Analyses were conducted separately in each hemisphere. Corticopontine projections are known to be exclusively ipsilateral and here we used an exclusion mask to terminate trajectories that crossed the midline.

These analyses resulted in seven probability distribution maps of the cerebral peduncle, one for each cortical zone. These were integrated into a single representation by assigning each voxel in the source mask with the identity of the cortical zone most likely to project to it. The size and spatial location of projections from each of the cortical areas was most easily visualized in this integrated representation ('hard segmentation'; see Fig. 1 and Fig. S1 in Supplementary Material).

Variability Maps of Tracts

The same methods enabled us to determine the trajectory of pathways in a probabilistic manner. The trajectories of non-zero probability values between the relevant segment of the cerebral peduncle (calculated as above) and cortex were mapped, thresholded (voxels with a probability of 10% or less were excluded) and registered into the coordinate stereotaxic space defined by the ICBM template brain (Jenkinson M *et al.*, 2002). Binary representations of registered, thresholded tracts from each subject were summed to create a probabilistic map that showed the case-to-case anatomical variability of the tracts. In order to determine the voxels in which this tract was present in most subjects, we applied a threshold of 5/9 cases to these maps (thus only including voxels in which PDFs were present in a majority of cases). This information allowed us to determine the areas from which tracts most commonly originated in each cortical area of interest, and also the most common trajectory taken by tracts from each of the seven cortical areas of interest through the white matter to the cerebral peduncles.

Statistical Analysis Of Hard Segmentation In Human Cases

Statistical analysis was conducted in SPSS (11.5). The percentage of the cerebral peduncle mask that each segment occupied was calculated, and a repeated-measures analysis of variance (ANOVA) was performed in which one factor was cortical area from which fibres originated (seven levels, one for each cortical zone), and the other was laterality (two levels: left or right hemisphere). The ANOVA table is reported in full in table S1. In order to assess the extent to which the relative size of each peduncle segment differed from the others, multiple pairwise comparisons were conducted with a post-hoc Bonferroni test (reported in full in Table S2).

Results

We subdivided the cortex into seven areas (see Fig. 1; see also Supplementary Material for anatomical criteria used to segment the prefrontal, premotor, primary motor, somatosensory, parietal, visual cortices and the temporal lobe). We defined the boundary between the prefrontal cortex and the premotor cortex in the precentral sulcus in the human brain and in the arcuate sulcus in the macaque monkey brain. We also identified the external segment of the cerebral peduncle in each hemisphere. Only sections below the thalamus were selected to avoid contributions from the cortico-thalamic system to any tracts defined in our study. Our aim was to segment the cerebral peduncle into areas that received fibres from each of the seven ipsilateral cortical areas. DT-MRI cannot distinguish between efferent and afferent fibres, but the cerebral peduncles are known to contain fibres that project from the cortex to the pontine nuclei.

Tractographic methods have been applied to diffusion images to estimate the path of least resistance to diffusion from seed regions. Previously employed fibre tracking methods have parcellated white matter using such 'streamlining' approaches (Huang *et al.*, 2005); for example, have parcellated the corpus callosum on the basis of areas of fibre origin in the cortex. Our statistical approach used Bayesian principles that quantified the probability that a tract from a particular part of the cortex ran though a given voxel (Behrens *et al.*, 2003a,b). Each voxel in the cerebral peduncle could therefore be automatically assigned a probability reflecting the likelihood that a tract propagated from it to any defined neocortical area. This analysis was repeated for each cortical area. The relative contributions of projections from different cortical areas to the cerebral peduncle could be visualized by assigning to each cerebral peduncle voxel the identity of the cortical area most likely to project through it ('hard segmentation'; see Fig. 1*D–G*).

We found a clear topographic organization in the cerebral peduncles in humans and macaque monkeys that is highly consistent with the classical view of the organization of corticopontine fibres within the cerebral peduncle. Fibres from cortical motor areas (primary and premotor cortex) were flanked anteriorly by representation of prefrontal fibres and posteriorly by those originating in the parietal cortex. Those from visual cortex and temporal lobe were negligible in humans and macaques. Figure 1*A–C* shows the cortical parcellation scheme (although this should not be taken to infer that fibres were found to originate uniformly from the whole of each region). Figure 1*D–G* shows the resulting segmentation of the cerebral peduncle (see also Supplementary Material for results from all cases).

Our results confirm that in macaque monkeys the cortical motor areas make the most significant contribution to the anatomical architecture of the cortico-ponto-cerebellar system. The contribution of the prefrontal cortex was found to be substantially smaller and originated predominantly in tissue above the dorsal bank of sulcus principalis in the dorsal prefrontal cortex (see Fig. 2*D*), as found in studies using conventional anatomical tracers (Schmahmann and Pandya, 1997). This area is also the principal prefrontal area that projects to the cortical motor system via the premotor cortex

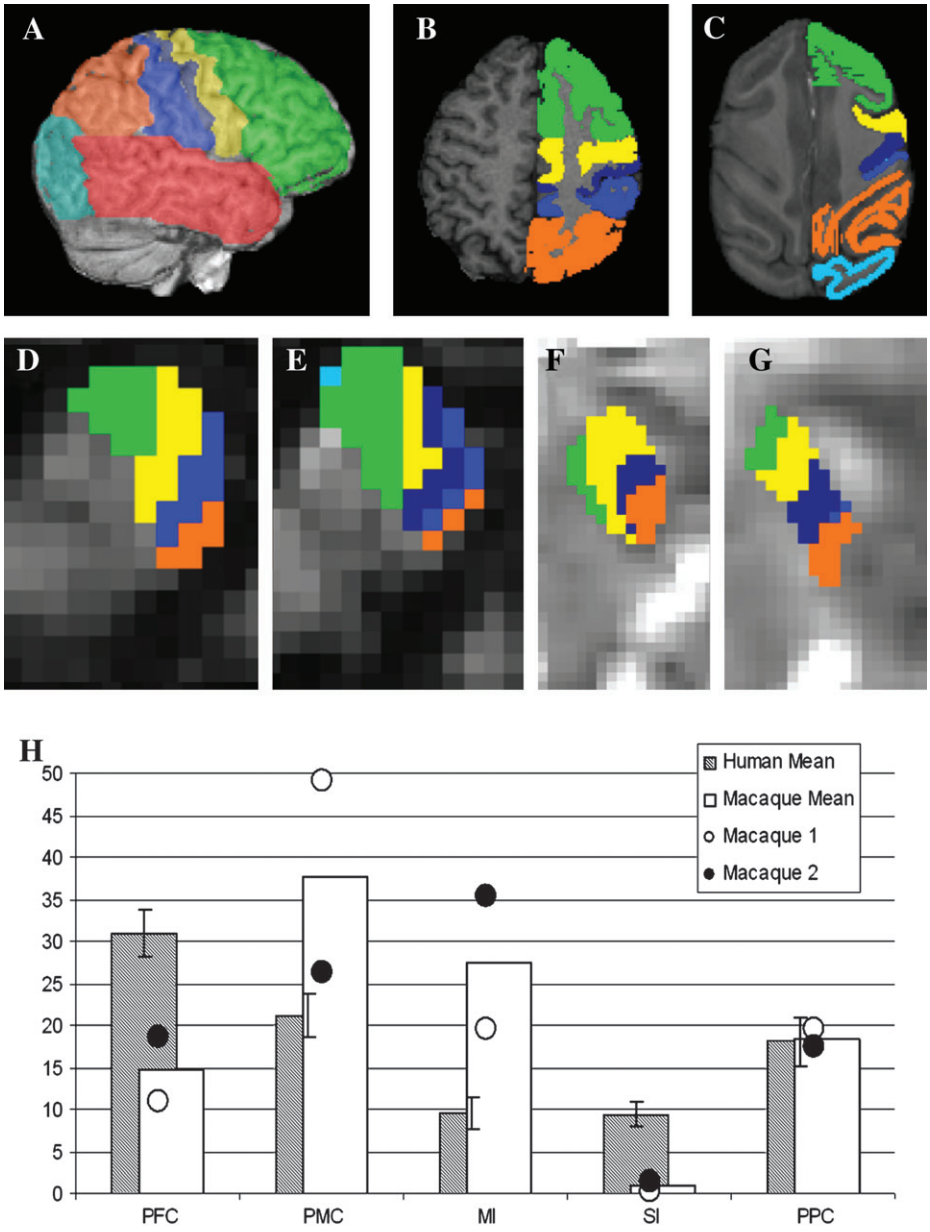

Figure 1. Schematic illustration of cortical areas used for delineation of projections from the cerebral peduncle in the human brain (3D rendering) (*A*), in axial section (*B*) and in the macaque monkey (*C*; axial section). Anterior–posterior: green, prefrontal cortex (pfc); yellow, premotor cortex (pmc); dark blue, primary motor cortex (M1); light blue, somatosensory cortex (S1 and S2); orange, posterior parietal cortex (ppc); cyan, visual cortex (vis); red, temporal lobe (TL). Parcellation of the right cerebral peduncle using DT-MRI in two representative human cases (*D*, *E*) and two monkey cases (*F*, *G*) showing hard segmentations (coloured according to *A* and *B*) of fibres from cortical areas overlaid on the cerebral peduncles (grey). (*H*) Graph showing the percentage of the cerebral peduncle area occupied by segments of fibres from different cortical areas (*y*-axis): hatched bars, human cases (left and right averaged); white bars, averaged monkey cases (right hemisphere); white circle, monkey 1; black circle, monkey 2. Temporal lobe and visual cortex representations were negligible and were not included in the graphs.

in monkeys (Lu *et al.*, 1994). Our results therefore demonstrate that diffusion imaging can be reliably used to map the pathways within the cortico-ponto-cerebellar system and that it generates connectivity patterns comparable with those found using conventional methods in the same species.

The same relative topographic organization was found consistently in all 18 human hemispheres, with tracts from cortical motor areas flanked anteriorly by a prefrontal representation and posteriorly by a parietal representation. As in the macaque monkey cases, contributions from temporal lobe and visual cortex were minor or absent. The proportional contributions of fibres in the human cases were assessed using a repeated-measures ANOVA (see Table S1). They differed significantly depending on the cortical areas of origin [repeated-measures ANOVA, main effect of cortical zone: $F(1,8) = 61.42$, $P < 0.005$; see Fig. 1). In order to determine which cortical areas contributed to this main effect, we used planned *post hoc* pairwise comparisons (Bonferroni corrected for multiple comparisons; see Table S2 for all pairwise comparisons). We found that contributions from the prefrontal cortex were larger than those from all areas ($P < 0.05$) except the premotor and parietal cortex ($P > 0.05$). We also used a *t*-test for

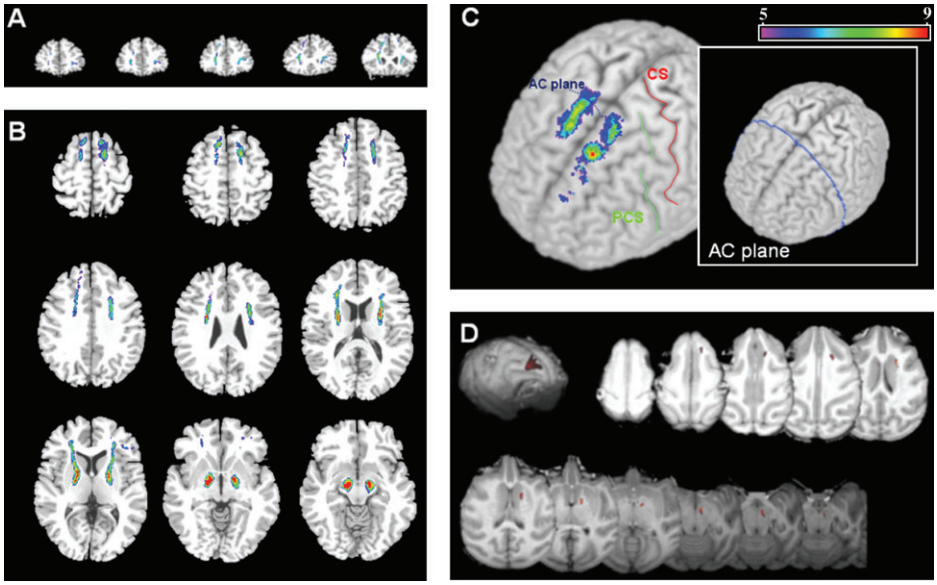

Figure 2. Course of fibre tracts from the prefrontal cortex to the cerebral peduncles. The right side of the brain is depicted on the right side of the image. Tracts generated in human cases were spatially registered into a common stereotaxic coordinate system and rendered onto the canonical brain of the ICBM series (see Materials and Methods). (*A*) The figure shows the map conservatively thresholded at 5/9 cases (i.e. showing voxels in which tracts were present in at least 5/9 cases). (*A*) Coronal sections through the human prefrontal cortex (left–right, anterior–posterior). (*B*) Axial sections through the human brain, showing probabilistic tract representations passing through the cerebral peduncle (top left–bottom right, dorsal–ventral). (*C*) Origin of tracts from the human prefrontal cortex in both hemispheres; blue line, plane of the anterior commissure passing through the superior frontal gyrus; green line, precentral sulcus; red line, central sulcus; inset, coronal plane of the anterior commissure). Colour bar for *A*, *B* and *C*: range, 5–9 cases. (*D*) Path of principle diffusion function from the macaque monkey prefrontal cortex to the cerebral peduncle. The origin of the path appears in the dorsal prefrontal cortex in tissue above sulcus principalis (3D rendered brain). The path travels through the anterior limb of the internal capsule and terminates in the medial sector of the cerebral peduncle (serial axial sections; dorsal to ventral represented left to right).

inter-species comparisons of results from the prefrontal and premotor cortex of humans and macaque monkeys. The relative prefrontal contribution to the cerebral peduncle in macaque monkeys was significantly smaller than that found in the human cases (*t*-test; $t = 2.782$, $P < 0.05$). In contrast, the relative contribution of the premotor cortex was significantly larger in the macaque monkeys compared with humans (*t*-test; $t = -2.715$, $P < 0.05$). Our measurements show that the enlargement in the fraction of the cerebral peduncles carrying prefrontal tracts between macaque monkeys and humans (monkeys, 14.76%; humans, 30.85%) is approximately matched with the corresponding enlargement in the grey matter volume of the prefrontal cortex (monkeys, 16.4 ± 0.3%; humans, 29.28 ± 2.37%). This is consistent with the view that the evolutionary pressures driving the expansion of the prefrontal cortex are also acting on the cerebral peduncles.

The volumes occupied by tracts from left and right hemispheres from each of the cortical areas were not significantly different from each other [no main effect of laterality; ANOVA, $F(1,8) = 0.056$, $P > 0.005$]. There were no significant differences in laterality related to individual cortical areas [ANOVA, Laterality × Cortical Zone interaction: $F(1,8) = 0.335$, $P > 0.005$].

In contrast to the human cases, the relative volumes occupied by tracts from cortical motor areas were larger than those of other areas in the macaque monkey cases. Cortical motor inputs to the cerebral peduncle are composed of direct cortico-spinal projections that bypass the pontine nuclei, their collaterals which project to the pontine nuclei, and direct cortico-pontine projections that do not contribute to cortico-spinal fibres. In our study, it was not possible to dissociate cortico-pontine from cortico-spinal tract representations. However, it has been estimated that only ~5.3% of fibres in the human cerebral peduncle project to the cortico-spinal tract (Tomasch, 1969), so the majority of fibres in the cerebral peduncle must be cortico-pontine.

In the human cases, tracts from the prefrontal cortex were registered into a common anatomical frame of reference so that the trajectories that were most consistent between members of the group could be determined (Fig. 2*A–C*). The most consistent origin for fibres from the prefrontal cortex was the superior frontal gyrus. All of the prefrontal cortical points of origin lay anterior to precentral sulcus. Most of these were also anterior to the coronal plane of the anterior commissure (AC plane; see inset of Fig. 2*C*), a more conservative landmark for the border between prefrontal and premotor cortex (Vorobiev *et al.*, 1998). Prefrontal areas of origin for fibre tracts contributing to the cerebral peduncle also were also noted in the inferior frontal gyrus and the frontal pole (see Fig. 2*B*), but these were much less prominent. After their origins, the anatomical white matter paths traced were very similar in the human and macaque brains, descending from prefrontal cortex into the anterior limb of the internal capsule, progressing ventrally between the caudate and putamen before passing through medial segments of the cerebral peduncle.

The estimated contributions of the prefrontal cortex and premotor cortex to fibres in the cerebral peduncle may depend on the precise location of the boundary between these cortical areas. In the macaque monkey, this boundary is reliably demarcated by the arcuate sulcus — a clearly identifiable gross morphological landmark. Petrides and Pandya (1999) report that the borders between area 6 (classically regarded as premotor cortex) and immediately anterior cytoarchitectonic territories of the prefrontal cortex (the subregions of area 8) lie in the depths of the arcuate sulcus. Petrides and Pandya (2002)

have therefore included all areas anterior to the arcuate sulcus into the macaque monkey prefrontal cortex. We also adopt this criterion. Its human homologue, the precentral sulcus, also marks the approximate boundary in the human brain, but its coincidence with the boundary between the cytoarchitectonic areas is not as well established and may be less reliable. However, it has been argued on the basis of neurodevelopmental branching of the precentral sulcus that the inferior portion of the arcuate sulcus in the monkey corresponds to the ascending branch of human inferior precentral sulcus plus inferior frontal sulcus and that superior portion of the arcuate sulcus in the monkey corresponds to human superior precentral sulcus plus the superior frontal sulcus (Rizzolatti *et al.*, 1998). We have therefore adopted the precentral sulcus as the posterior border between the human prefrontal and premotor cortex. It is arguable that the relatively large prefrontal representations that we report in the cerebral peduncle may in fact contain a significant proportion of fibres from the premotor cortex. In a recent methodological paper (Lazar and Alexander, 2005) the boundary was placed at a more anterior location ($y = 0$ in MNI standard space, corresponding to the coronal plane of the anterior commissure). They incidentally report a relatively small prefrontal contribution to the cerebral peduncle, which can probably be explained by artefacts caused by scanning at the high magnetic field strength used in their study (3T). We recalculated the relative proportions of prefrontal and premotor fibres in the cerebral peduncle when the border between the cortical masks was set at $y = 0$. The relative proportion of prefrontal fibres is slightly reduced in some subjects in comparison to Figure 1*H*. However, the average contributions of these areas remain largely the same (see Fig. S2 in Supplementary Material online). There is no statistically significant effect of changing the border definition on the size of the prefrontal and premotor representations in the cerebral peduncle [repeated-measures ANOVA, $F(1,8) = 0.036$, $P < 0.005$].

Discussion

Our study suggests that in the human brain there is a larger volume of white matter in the cerebral peduncle that arises in the prefrontal cortex than from other cortical areas. By contrast, in macaque monkeys, this system is relatively minor, with the overwhelming majority of projection fibres arising from cortical motor areas. We interpret this as evidence for a greater contribution of prefrontal fibres to the cortico-ponto-cerebellar system in humans. Our evidence is consistent with the suggestion that the human cortico-ponto-cerebellar system may have a specific role in processing higher level 'cognitive' information from the prefrontal cortex (Leiner *et al.*, 1986, 1991, 1993).

However, there are a number potential caveats to our interpretation of these results.

First, the achievable resolution of diffusion images and modelling limitations, along with the complex geometry of fibres in the pontine nuclei, currently preclude accurate tracing of fibres from the cortex directly into the cerebellum. We therefore focussed our investigation on cortical inputs to the cerebral peduncle — an important point through which all cortical projections to the cerebellum spatially converge into a small location in a highly organized manner. Although the cerebral peduncle includes a mixed projection bundle with descending fibres of the corticospinal tract as well as those in corticopontine system, the overwhelming majority of fibres contribute to the latter (Tomasch, 1969).

A second potential caveat is that the claim that there are a greater number of fibres arising in the human prefrontal cortex than from other areas can only be true if fibre density in anterior areas of the cerebral peduncle is the same as (or greater than) that in posterior parts. Histological analysis of the human cerebral peduncle reveals that the density of fibres is in fact greater in the anterior part of the cerebral peduncle than in posterior parts (Tomasch, 1969). This would argue that our results may even be *underestimating* the relative contribution of prefrontal projection fibres to the human cerebral peduncle.

Third, our study examines cortico-pontine fibres rather then the entire cortico-ponto-cerebellar system. It is therefore important to consider the assumptions we make in extending our arguments to the cortico-ponto-cerebellar system in general. It is widely recognized that nearly all neurons in the pontine nuclei project to the cerebellar cortex (Brodal and Bjaalie, 1992). Thus, it would be reasonable to assume that cortical inputs to the pontine nuclei, and pontine outputs to the cerebellar cortex convey prefrontal information in similar proportions. Although there is a theoretical possibility that the pontine nuclei receive large amounts of information from the prefrontal cortex but selectively filter this so that prefrontal information conveyed from the pontine nuclei to the cerebellum is reduced, we are not aware of any evidence that would support this.

The most posterior cytoarchitectonic area within the macaque prefrontal cortex is area 8 (Petrides and Pandya, 1999, 2002). Its posterior parts form a border with premotor area 6. Area 8 is well-known for its involvement in oculomotor control. Thus, although we draw an anatomical distinction between the prefrontal and premotor cortex, we do not mean to draw absolute functional distinctions between exclusively cognitive operations in the prefrontal cortex and exclusively motor functions in the premotor cortex. Clearly posterior parts of the prefrontal cortex, such as area 8, are engaged in the control of action and therefore share functional properties with adjacent parts of the premotor cortex. It might be argued that in the human brain, prefrontal contributions to the cortico-pontine system might arise mostly from these areas rather than more anterior areas. It is therefore important to consider the possibility that the relative contributions of fibres from the prefrontal and premotor cortex could depend on where the location of the border between these areas is placed in the frontal lobes. The arcuate sulcus reliably coincides with this border in the macaque monkey, but the human homologue of this landmark (precentral sulcus) is a less dependable cytoarchitectonic landmark. We directly tested whether the apparent size of the prefrontal zone in the cerebral peduncle decreases significantly with small changes in the cortical target borders between premotor and prefrontal cortices by adopting the coronal plane of the anterior commissure as an alternative border and re-analysing our data. This made no statistically significant difference to the sizes of the prefrontal and premotor areas in the cerebral peduncle (see Supplementary Material). The findings therefore are robust to reasonable uncertainty in the relationship between neocortical cytoarchitecture and the borders between target masks chosen.

A final potential caveat relates to the potential for biases inherent in DT-MRI to influence our results. It might be argued that tracking is less efficient from relatively small locations such

as the cerebral peduncle that contain fewer voxels than some of the much larger areas to which our methods have been applied (Behrens *et al*., 2003a,b; Johansen-Berg *et al*., 2004, 2005). One of the most important factors to influence the ability to track fibres is the level of organization within the pathway being investigated. Probabilistic estimates of anisotropy are high in large, geometrically simple, well-organized fibre systems such as the cerebral peduncle. Consequently this makes the fibres in the cerebral peduncle much easier to track than most other fibre systems in the brain even if the sources of fibres in these other fibre systems contain more voxels. The efficiency of fibre tracking is also influenced by factors such as the tendency for information to be degraded by image artefacts in some areas more than others, the distance of source area from the target area, and the fact that it is increasingly difficult to trace tracts with greater curvature or tracts interrupted by crossing fibres. However, the relatively large representation of prefrontal fibres in the human cerebral peduncle cannot be explained by these factors. Tracts from the prefrontal cortex (particularly the frontal pole) are in fact longer than those from other areas and tracts from other cortical areas experience less curvature (the exception to this is the temporal lobe, but our pilot studies showed that manipulating the curvature threshold does not influence the ability to detect temporal lobe fibres), suggesting that these biases also should lead only to underestimation of prefrontal contributions.

Our study makes three new contributions to understanding of the cortico-pontine component of the cortico-ponto-cerebellar system. First, we provide novel anatomical evidence from the human brain that there is a major contribution from the prefrontal cortex to the pontine nuclei. Unlike previous studies that have relied on lesion-related degeneration of fibre tracts (Beck, 1950; Marin *et al*., 1962; Schultz *et al*., 1976), we have been able to determine the extent of contributions from all cortical areas simultaneously and bilaterally in the same brains. In doing so, we demonstrate that DT-MRI can define the intrinsic organization of fibres within white matter tracts of the human brain quantitatively in-vivo.

Second, the parallel studies in the macaque monkey help to validate the tractographic methodology with respect to conventional, invasive tract-tracing approaches, giving us confidence in the new anatomical data. Conventional anatomical methods have enabled the detailed characterization of the macaque cortico-ponto-cerebellar system (Brodal, 1978, 1979; Glickstein *et al*., 1980, 1985, 1994; Matelli *et al*., 1984; Schmahmann and Pandya, 1991, 1992, 1995, 1997; Middleton and Strick, 2001; Kelly and Strick, 2003), allowing us to predict clearly not only its topographical organization but also the dominant contribution of the cortical motor system in this species. The automatic parcellation of the white matter in the macaque monkey cerebral peduncles into an expected topographic structure confirms classical descriptions of its organization. By applying the same methods of investigation in two different species we also have been able to directly address an important comparative anatomical hypothesis suggesting the evolution of functional circuitry as a whole rather than simply the evolution of individual brain areas (Barton and Harvey, 2000).

Third, we report novel findings about the organization of the human cortico-ponto-cerebellar system. The results reveal substantial growth of prefrontal projections that complement the evolutionary expansion seen in the human prefrontal cortex and ventral dentate nucleus in the human cerebellum (Dow, 1942; Matano, 2001). Our evidence supports the view that selectional pressures that bring about brain evolution do so by acting on interconnected systems rather than simply on individual brain areas (Barton and Harvey, 2000). This suggests that the human cerebellum may play specialized roles in processing cognitive information. A future challenge is to determine how specific areas within the prefrontal cortex contribute to the cortico-ponto-cerebellar system.

Supplementary Material

Supplementary Material can be found at: http://www.cercor.oxfordjournals.org/

Notes

We would like to thank Dr Claudia Wheeler-Kingshott, Dr. Phil Boulby and Prof. Gareth Barker for their contributions to acquiring the human diffusion data. Our work is supported by The Wellcome Trust (H.J.B., O.C.), the UK Medical Research Council (N.R., H.J.B., T.E.J.B., P.R., P.M.M.), the National Institute of Health (C.G.), the National Institute of Mental Health (S.K.) and the Whitehall Foundation (S.K.). The scanner in the NMR unit is sponsored by the MS Society of Great Britain and Northern Ireland (A.T.). We are grateful to Prof. Chris Frith for helpful comments on an earlier draft of the manuscript.

Address correspondence to Dr Narender Ramnani, Cognitive Neuroscience Laboratory, Department of Psychology, Royal Holloway University of London, Egham, Surrey TW20 0EX, UK. Email: n.ramnani@rhul.ac.uk.

References

Andersson J, Richter M, Richter W, Skare S, Nunes R, Robson M, TEJ Behrens (2004) Effects of susceptibility distortions on tractography. In: ISMRM, Kyoto.

Barton RA, Harvey PH (2000) Mosaic evolution of brain structure in mammals. Nature 405:1055–1058.

Beck E (1950) The origin, course and termination of the prefronto-pontine tract in the human brain. Brain 73:368–391.

Behrens TE, Johansen-Berg H, Woolrich MW, Smith SM, Wheeler-Kingshott CA, Boulby PA, Barker GJ, Sillery EL, Sheehan K, Ciccarelli O, Thompson AJ, Brady JM, Matthews PM (2003a) Non-invasive mapping of connections between human thalamus and cortex using diffusion imaging. Nat Neurosci 6:750–757.

Behrens TE, Woolrich MW, Jenkinson M, Johansen-Berg H, Nunes RG, Clare S, Matthews PM, Brady JM, Smith SM (2003b) Characterization and propagation of uncertainty in diffusion-weighted MR imaging. Magn Reson Med 50:1077–1088.

Brodal P (1978) The corticopontine projection in the rhesus monkey. Origin and principles of organization. Brain 101:251–283.

Brodal P (1979) The pontocerebellar projection in the rhesus monkey: an experimental study with retrograde axonal transport of horseradish peroxidase. Neuroscience 4:193–208.

Brodal P, Bjaalie JG (1992) Organization of the pontine nuclei. Neurosci Res 13:83–118.

Brodal P, Bjaalie JG (1997) Salient anatomic features of the cortico-ponto-cerebellar pathway. Prog Brain Res 114:227–249.

Dow RS (1942) The evolution and anatomy of the cerebellum. Rev Camb Philos Soc 17:179–220.

Finlay BL, Darlington RB (1995) Linked regularities in the development and evolution of mammalian brains. Science 268:1578–1584.

Glickstein M (1993) Motor skills but not cognitive tasks. Trends Neurosci 16:450–451.

Glickstein M, Cohen JL, Dixon B, Gibson A, Hollins M, Labossiere E, Robinson F (1980) Corticopontine visual projections in macaque monkeys. J Comp Neurol 190:209–229.

Glickstein M, May JG, 3rd, Mercier BE (1985) Corticopontine projection in the macaque:the distribution of labelled cortical cells after large injections of horseradish peroxidase in the pontine nuclei. J Comp Neurol 235:343–359.

Glickstein M, Gerrits N, Kralj-Hans I, Mercier B, Stein J, Voogd J (1994) Visual pontocerebellar projections in the macaque. J Comp Neurol 349:51–72.
Huang H, Zhang J, Jiang H, Wakana S, Poetscher L, Miller MI, van Zijl PC, Hillis AE, Wytik R, Mori S (2005) DTI tractography based parcellation of white matter: application to the mid-sagittal morphology of corpus callosum. Neuroimage 26:195–205.
Jenkinson M, Bannister P, Brady J, Smith S (2002) Improved optimisation for the robust and accurate linear registration and motion correction of brain images. Neuroimage 17:825–841.
Johansen-Berg H, Behrens TE, Robson MD, Drobnjak I, Rushworth MF, Brady JM, Smith SM, Higham DJ, Matthews PM (2004) Changes in connectivity profiles define functionally distinct regions in human medial frontal cortex. Proc Natl Acad Sci USA 101:13335–13340.
Johansen-Berg H, Behrens TE, Sillery E, Ciccarelli O, Thompson AJ, Smith SM, Matthews PM (2005) Functional–anatomical validation and individual variation of diffusion tractography-based segmentation of the human thalamus. Cereb Cortex 15:31–39.
Jones DK, Horsfield MA, Simmons A (1999) Optimal strategies for measuring diffusion in anisotropic systems by magnetic resonance imaging. Magn Reson Med 42:515–525.
Kelly RM, Strick PL (2003) Cerebellar loops with motor cortex and prefrontal cortex of a nonhuman primate. J Neurosci 23:8432–8444.
Lazar M, Alexander AL (2005) Bootstrap white matter tractography (BOOT-TRAC). Neuroimage 24:524–532.
Leiner HC, Leiner AL, Dow RS (1986) Does the cerebellum contribute to mental skills? Behav Neurosci 100:443–454.
Leiner HC, Leiner AL, Dow RS (1991) The human cerebro-cerebellar system:its computing, cognitive, and language skills. Behav Brain Res 44:113–128.
Leiner HC, Leiner AL, Dow RS (1993) Cognitive and language functions of the human cerebellum. Trends Neurosci 16:444–447.
Lu MT, Preston JB, Strick PL (1994) Interconnections between the prefrontal cortex and the premotor areas in the frontal lobe. J Comp Neurol 341:375–392.
Marin OSM, Angevine JB, Locke S (1962) Topographical organisation of the lateral segment of the basis pedunculi in man. J Comp Neurol 118:165–175.
Matano S (2001) Brief communication: proportions of the ventral half of the cerebellar dentate nucleus in humans and great apes. Am J Phys Anthropol 114:163–165.
Matelli M, Camarda R, Glickstein M, Rizzolatti G (1984) Interconnections within the postarcuate cortex (area 6) of the macaque monkey. Brain Res 310:388–392.
Middleton FA, Strick PL (1994) Anatomical evidence for cerebellar and basal ganglia involvement in higher cognitive function. Science 266:458–461.
Middleton FA, Strick PL (1997) Dentate output channels:motor and cognitive components. Prog Brain Res:114553–114566.
Middleton FA, Strick PL (2000) Basal ganglia and cerebellar loops:motor and cognitive circuits. Brain Res Brain Res Rev 31:236–250.
Middleton FA, Strick PL (2001) Cerebellar projections to the prefrontal cortex of the primate. J Neurosci 21:700–712.
Munger P, Crelier GR, Peters TM, Pike GB (2000) An inverse problem approach to the correction of distortion in EPI images. IEEE Trans Med Imag 19:681–689.
Orioli PJ, Strick PL (1989) Cerebellar connections with the motor cortex and the arcuate premotor area:an analysis employing retrograde transneuronal transport of WGA-HRP. J Comp Neurol 288:612–626.
Petrides M, Pandya DN (1999) Dorsolateral prefrontal cortex:comparative cytoarchitectonic analysis in the human and the macaque brain and corticocortical connection patterns. Eur J Neurosci 11:1011–1036.
Petrides M, Pandya DN (2002) Comparative cytoarchitectonic analysis of the human and the macaque ventrolateral prefrontal cortex and corticocortical connection patterns in the monkey. Eur J Neurosci 16:291–310.
Pinsk MA, Moore T, Richter MC, Gross CG, Kastner S (2005) Methods for functional magnetic resonance imaging in normal and lesioned behaving monkeys. J Neurosci Methods (in press).
Rilling JK, Insel TR (1998) Evolution of the cerebellum in primates: differences in relative volume among monkeys, apes and humans. Brain Behav Evol 52:308–314.
Rizzolatti G, Luppino G, Matelli M (1998) The organization of the cortical motor system:new concepts. Electroencephalogr Clin Neurophysiol 106:283–296.
Schmahmann JD, Pandya DN (1991) Projections to the basis pontis from the superior temporal sulcus and superior temporal region in the rhesus monkey. J Comp Neurol 308:224–248.
Schmahmann JD, Pandya DN (1992) Course of the fiber pathways to pons from parasensory association areas in the rhesus monkey. J Comp Neurol 326:159–179.
Schmahmann JD, Pandya DN (1995) Prefrontal cortex projections to the basilar pons in rhesus monkey:implications for the cerebellar contribution to higher function. Neurosci Lett 199:175–178.
Schmahmann JD, Pandya DN (1997) Anatomic organization of the basilar pontine projections from prefrontal cortices in rhesus monkey. J Neurosci 17:438–458.
Schultz W, Montgomery EB, Marini R (1976) Stereotyped flexion of forelimb and hindlimb to microstimulation of dentate nucleus in cebus monkeys. Brain Res 107:151–151.
Smith SM (2002) Fast robust automated brain extraction. Hum Brain Mapp 17:143–155.
Tomasch J (1969) The numerical capacity of the human cortico-pontocerebellar system. Brain Res 13:476–484.
Vorobiev V, Govoni P, Rizzolatti G, Matelli M, Luppino G (1998) Parcellation of human mesial area 6: cytoarchitectonic evidence for three separate areas. Eur J Neurosci 10:2199–2203.
Wheeler-Kingshott CAM, Boulby PA, Symms M, Barker GJ (2002) Optimised cardiac gating for high-resolution whole-brain DTI on a standard scanner. Proc Intl Mag Reson Med:1118.
Zhang Y, Brady M, Smith S (2001) Segmentation of brain MR images through a hidden Markov random field model and the expectation maximization algorithm. IEEE Trans Med Imag 20:45–57.
Zilles K, Armstrong E, Schleicher A, Kretschmann HJ (1988) The human pattern of gyrification in the cerebral cortex. Anat Embryol (Berl) 179:173–179.
Zilles K, Armstrong E, Moser KH, Schleicher A, Stephan H (1989) Gyrification in the cerebral cortex of primates. Brain Behav Evol 34:143–150.